# Salt-inducible kinase 2 links transcriptional coactivator p300 phosphorylation to the prevention of ChREBP-dependent hepatic steatosis in mice

Julien Bricambert,[1,2] Jonatan Miranda,[1,2,3] Fadila Benhamed,[1,2] Jean Girard,[1,2] Catherine Postic,[1,2] and Renaud Dentin[1,2]

[1]Institut Cochin, Département d'Endocrinologie, Métabolisme et Cancer, Université Paris Descartes, CNRS, UMR 8104, INSERM, U1016, Paris, France. [2]INSERM, U1016, Paris, France. [3]Department of Nutrition and Food Science, University of País Vasco, Vitoria, Spain.

**Obesity and type 2 diabetes are associated with increased lipogenesis in the liver. This results in fat accumulation in hepatocytes, a condition known as hepatic steatosis, which is a form of nonalcoholic fatty liver disease (NAFLD), the most common cause of liver dysfunction in the United States. Carbohydrate-responsive element–binding protein (ChREBP), a transcriptional activator of glycolytic and lipogenic genes, has emerged as a major player in the development of hepatic steatosis in mice. However, the molecular mechanisms enhancing its transcriptional activity remain largely unknown. In this study, we have identified the histone acetyltransferase (HAT) coactivator p300 and serine/threonine kinase salt-inducible kinase 2 (SIK2) as key upstream regulators of ChREBP activity. In cultured mouse hepatocytes, we showed that glucose-activated p300 acetylated ChREBP on Lys672 and increased its transcriptional activity by enhancing its recruitment to its target gene promoters. SIK2 inhibited p300 HAT activity by direct phosphorylation on Ser89, which in turn decreased ChREBP-mediated lipogenesis in hepatocytes and mice overexpressing SIK2. Moreover, both liver-specific SIK2 knockdown and p300 overexpression resulted in hepatic steatosis, insulin resistance, and inflammation, phenotypes reversed by SIK2/p300 co-overexpression. Finally, in mouse models of type 2 diabetes and obesity, low SIK2 activity was associated with increased p300 HAT activity, ChREBP hyperacetylation, and hepatic steatosis. Our findings suggest that inhibition of hepatic p300 activity may be beneficial for treating hepatic steatosis in obesity and type 2 diabetes and identify SIK2 activators and specific p300 inhibitors as potential targets for pharmaceutical intervention.**

## Introduction

The metabolic syndrome, which represents a collection of abnormalities including obesity, type 2 diabetes, dyslipidemia, fatty liver, and a proinflammatory state (1), affects more than 27% of adults in the United States (2) and has become a major health concern worldwide. Central to the pandemic of this disease cluster is the dramatic increase in the incidence of obesity in most parts of the world. Obesity-induced ectopic accumulation of fat activates cellular stress signaling and inflammatory pathways (3, 4), contributing to enhanced muscle insulin resistance, pancreatic β-cell failure, nonalcoholic steatohepatitis (NASH), and finally to organ damage. Of particular importance, increased fatty acid synthesis through the lipogenic pathway in liver results in the development of hepatic steatosis and contributes to the development of chronic hepatic inflammation and insulin resistance (reviewed in ref. 5).

Today, it is well accepted that chromatin organization and transcriptional regulation are major components of the regulatory pathway where gene-specific transcription factors, coactivators, and corepressors interact which each other and with posttranslational modifiers to induce transcription. In particular, the capacity of the liver to regulate the expression of glycolytic and lipogenic genes, including L-pyruvate kinase (*L-PK*), fatty acid synthase (*Fas*), and acetyl-CoA carboxylase (*Acc*), to increase fatty acid synthesis in response to glucose and insulin is governed by a highly dynamic transcriptional regulatory network, including both SREBP-1c and carbohydrate-responsive element–binding protein (ChREBP) (6). ChREBP, which has recently emerged as the major mediator of glucose action on glycolysis and lipogenesis, acts in synergy with SREBP-1c to fully induce fatty acid synthesis (7, 8). Recent reports demonstrate that ChREBP plays an important role in the development of hepatic steatosis, since its liver-specific inhibition decreased the rate of hepatic lipogenesis and improved hepatic steatosis and insulin resistance in obese *ob/ob* mice (9, 10). Although ChREBP activity is partially regulated by phosphorylation (reviewed in ref. 6), the molecular mechanisms enhancing its transcriptional activity in obesity and type 2 diabetes states remain largely unknown.

Increasing evidence suggests that specific posttranslational marks on the histones and non-histone proteins, such as phosphorylation, acetylation, or methylation marks, may contribute to the regulation of glucose and lipid metabolism (11). These posttranslational marks are altered by histone-modifying enzymes, such as histone deacetylases (HDACs) and histone acetyltransferases (HATs) (12). Among the HAT family members, the transcriptional coactivator p300 is an important component of the transcriptional machinery that participates in the regulation of chromatin organization and transcription initiation (reviewed in

**Conflict of interest:** The authors have declared that no conflict of interest exists.
**Citation for this article:** *J Clin Invest.* 2010;120(12):4316–4331. doi:10.1172/JCI41624.

ref. 13). p300 takes part in diverse biological pathways, including differentiation, development, and proliferation (14, 15), and has been implicated in numerous disease processes, including several forms of cancers and cardiac hypertrophy (16, 17). Orchestration of these activities by p300 involves an enzymatic activity through a HAT domain for histone H3 and H4 acetylation and several other substrates including transcriptional regulators, resulting in enhanced gene transcription (18, 19). Since, p300 activity is also regulated via phosphorylation, it is believed that p300 HAT activity is a central integrator of various signaling pathways in the nucleus (20, 21). However, it is still unclear which kinases are responsible for p300 phosphorylation in vivo and where the phosphorylation occurs. More important, the functional links between specific phosphorylation events and p300 activity remain largely unknown, in particular the function of p300 in normal or aberrant regulation of fatty acid synthesis.

In the present study, we show that the serine/threonine kinase salt-inducible kinase 2 (SIK2), recently identified as a new AMPK/SNF1 family member (22), directly regulates hepatic lipogenesis through the regulation of p300 transcriptional activity by phosphorylation. First, we found that inhibition of SIK2 expression led to the development of hepatic steatosis characterized by an increase in de novo lipogenesis. This was due in part to enhanced ChREBP transcriptional activity by acetylation at Lys672, which increased its binding on its target gene promoters. We described SIK2 as an important inhibitor of p300 function through the inhibition of its HAT activity by direct phosphorylation at Ser89. More specifically, loss of SIK2 activity enhanced p300 HAT activity, which in turn increased ChREBP acetylation both in vitro and in vivo and potently stimulated ChREBP-induced transcription. Overall, our results demonstrate that hyperactivation of p300 HAT activity is responsible, at least in part, for increased ChREBP transactivation potency and for the development of hepatic steatosis in states of obesity and type 2 diabetes. These findings suggest that SIK2-dependent regulation of p300 function could be critical for the modulation of glucose and lipid homeostasis in obesity and insulin-resistance states.

## Results

*Liver-specific inhibition of SIK2 expression alters fatty acid metabolism and results in hepatic steatosis, insulin resistance, and inflammation*. Silencing SIK2 expression in liver (Figure 1A) enhanced the expression of gluconeogenic genes (*Pepck* and *G6Pase*) in the fed state (Figure 1G) by increasing CREB-regulated transcription coactivator 2 (CRTC2) activity through its dephosphorylation at Ser171 (Figure 1A and ref. 23). This resulted in the development of postprandial hyperglycemia, hyperinsulinemia (Figure 1C), insulin resistance (decreased Akt and FOXO1 phosphorylation and hepatic glycogen concentrations in fed mice injected with SIK2 shRNA adenovirus [SIK2i mice]) (Figure 1, A and D, and Supplemental Figure 1A), and glucose intolerance (Figure 1D), thus establishing the role of SIK2 in the regulation of hepatic glucose production and glucose homeostasis during feeding. Interestingly, SIK2 silencing also led to the development of hepatic steatosis characterized by an increase in liver weight (1.84 ± 0.23 g for mice injected with unspecific shRNA adenovirus [USi mice] vs. 3.74 ± 0.14 g for SIK2i mice) (Figure 1B). Histological analysis of liver sections from SIK2i mice revealed an increase in a mosaic pattern of hypertrophic hepatocytes showing abnormal accumulation of small cytoplasmic lipid droplets typical of a microvesicular steatosis, as revealed by oil red O staining (Figure 1B). Supporting this observation, both plasma and liver triglyceride (TG) levels were increased (Figure 1E). In addition, plasma concentrations of β-hydroxybutyrate, a marker of fatty acid oxidation and ketogenesis in the liver, were significantly lower in SIK2i mice despite the increase in plasma and liver FFA (non-esterified fatty acid [NEFA]) concentrations (Figure 1F and Supplemental Figure 1A). This observation is indicative of a cellular imbalance between fatty acid synthesis and fatty acid oxidation in the absence of SIK2. Consistent with the development of liver steatosis, mRNA levels of key genes involved in fatty acid synthesis (*L-PK*, ATP citrate lyase [*Acl*], *Acc*, and *Fas*) were significantly higher in the liver of SIK2i mice (Figure 1G) and correlated with a 70% increase in lipogenic rates (Figure 1B). Finally, no major change in the expression of genes involved in fatty acid oxidation (*Cpt1a*, *Ppara*, or *AOX*) was observed in liver of SIK2i mice (Supplemental Figure 1D), suggesting that the development of fatty liver in SIK2i mice mostly results from an increase in the lipogenic pathway. Excessive lipid accumulation in peripheral tissues is known to promote macrophage infiltration, thus stimulating local inflammation and eventually insulin resistance (24). mRNA analysis revealed 60% and 30% increases in the liver macrophage markers macrophage inflammation protein 1c (MIP1c) and F4/80+, respectively (Supplemental Figure 1D). In addition, several major proinflammatory cytokines, including resistin, TNF-α, and IL-6, were significantly increased in plasma of SIK2i mice (Supplemental Figure 1B). Plasma concentrations of the transaminases alanine aminotransferase (ALAT) and aspartate aminotransferase (ASAT) were also increased, suggesting early liver damage (Supplemental Figure 1C). Importantly, USi adenovirus injection in mice did not promote inflammation or liver damage compared with noninjected mice (data not shown). These observations indicate that inhibition of SIK2 expression in liver leads to the development of hepatic steatosis and inflammation, resulting in the development of insulin resistance.

Interestingly, while the transcriptional regulation of hepatic glycolytic and lipogenic genes is under the control of the transcription factors ChREBP and SREBP-1c, there was no significant change in the expression levels of these two transcriptional regulators in liver of SIK2i mice (Figure 1A and Supplemental Figure 1D), suggesting that SIK2 silencing enhances their transcriptional activity through posttranscriptional modification. In line with this hypothesis, it was recently reported that acetyl-CoA derived from glucose metabolism through the lipogenic pathway generates a substrate for chromatin modification and a signal for potentially activating glycolytic and lipogenic gene expression (25). To explore the molecular mechanism underlying altered liver function in SIK2i mice, we measured global histone acetylation in vivo by Western blot analysis (Figure 1H). We observed an increase in acetylation levels of histone H3K9 and H4K8, which was correlated with a significant increase in acetyl-CoA concentration (Figure 1H). Furthermore, increases in proximal H3K9 acetylation, ChREBP occupancy to its DNA response element (ChoRE), and RNA polymerase II recruitment were observed on the *L-PK* promoter in liver of SIK2i mice (Figure 1I). We next sought to determine whether this increase in acetyl-CoA content selectively affects acetylation of histones or has equivalent effects on the acetylation of other cellular proteins. Surprisingly, increasing acetyl-CoA content influenced acetylation of only a select set of substrates. In fact, we found that SIK2 silencing did not promote acetylation of tubulin, a cytoskeletal protein that is acetylated by the Elongator HAT complex (Figure

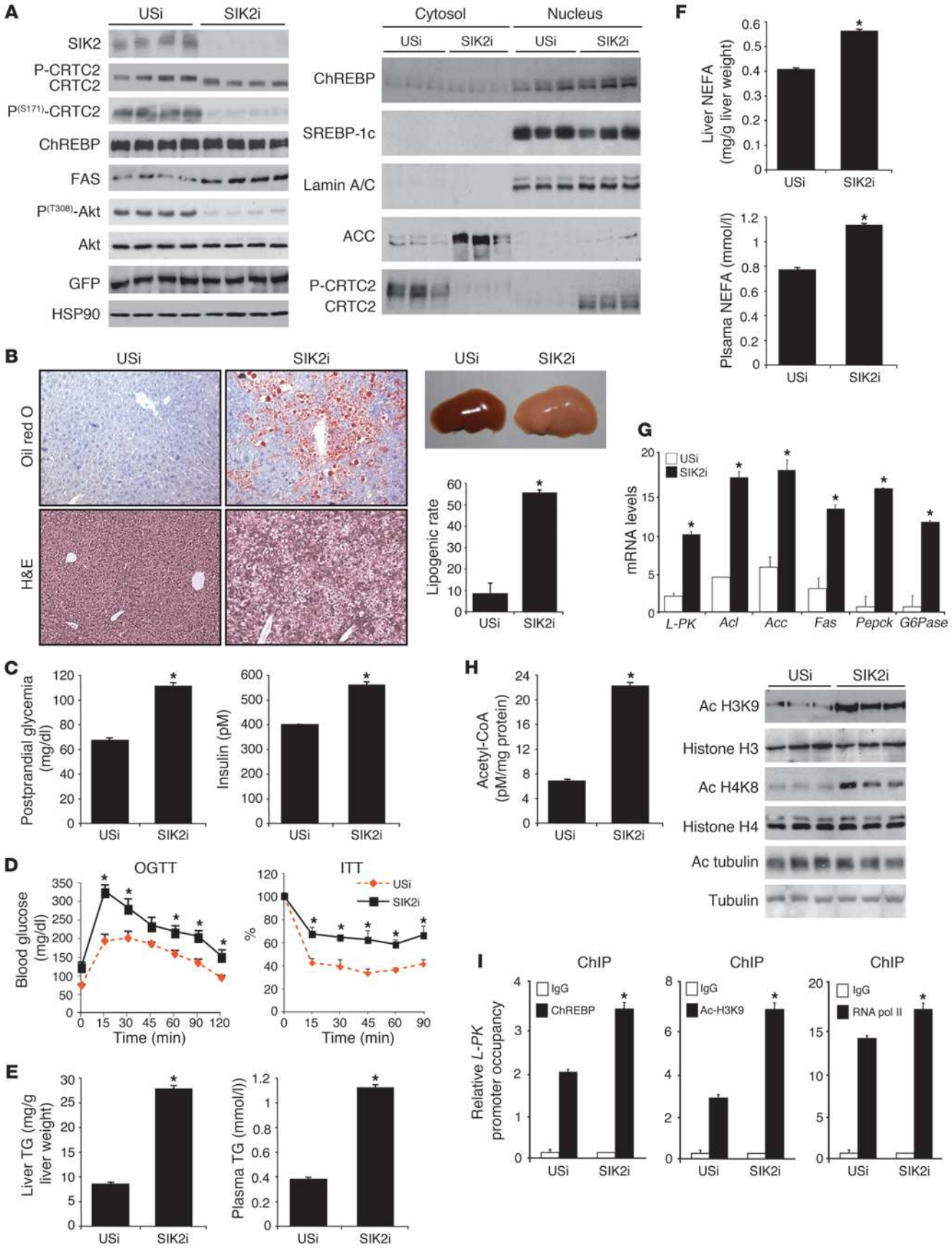
A
USi
SIK2i
SIK2
P-CRTC2
CRTC2
P(S171)-CRTC2
ChREBP
FAS
P(T308)-Akt
Akt
GFP
HSP90
Cytosol
Nucleus
ChREBP
SREBP-1c
Lamin A/C
ACC
P-CRTC2
CRTC2
F
Liver NEFA (mg/g liver weight)
Plsama NEFA (mmol/l)
B
Oil red O
H&E
Lipogenic rate
G
mRNA levels
L-PK
Acl
Acc
Fas
Pepck
G6Pase
C
Postprandial glycemia (mg/dl)
Insulin (pM)
D
OGTT
ITT
Blood glucose (mg/dl)
Time (min)
%
E
Liver TG (mg/g liver weight)
Plasma TG (mmol/l)
H
Acetyl-CoA (pM/mg protein)
Ac H3K9
Histone H3
Ac H4K8
Histone H4
Ac tubulin
Tubulin
I
ChIP
IgG
ChREBP
Ac-H3K9
RNA pol II
Relative L-PK promoter occupancy

**Figure 1**
Hepatic SIK2 silencing impairs lipid homeostasis. Mice were injected with unspecific (USi) or SIK2 shRNA adenovirus (SIK2i) and were studied 7 days later in the fed state. (**A**) Western blot analysis of key transcription factors and coactivators involved in the regulation of gluconeogenesis and lipogenesis in liver ($n$ = 3–4 per group). (**B**) SIK2i mice develop hepatic steatosis as shown by increased liver size and H&E and oil red O staining of liver sections and by the rate of lipogenesis. Original magnification, ×200 ($n$ = 4–8 per group; *$P$ < 0.05). (**C**) Plasma glucose and insulin levels ($n$ = 8 per group; *$P$ < 0.01). (**D**) OGTT and ITT ($n$ = 6 per group; *$P$ < 0.01). (**E** and **F**) Total liver and plasma TGs and FFA levels ($n$ = 8 per group; *$P$ < 0.01). (**G**) Relative expression of glycolytic, lipogenic, and gluconeogenic genes ($n$ = 8 per group; *$P$ < 0.01). (**H**) Acetyl-CoA concentrations ($n$ = 8 per group; *$P$ < 0.02) and amounts of acetylated (Ac) H3K9, H4K8, and tubulin determined by Western blot analysis ($n$ = 4 per group). (**I**) ChREBP, RNA polymerase II (RNA pol II) recruitment, and levels of acetylated H3K9 at the ChoRE-containing region of the *L-PK* promoter were measured by ChIP studies. The amount of immunoprecipitated H3 at the DNA was unchanged upon SIK2 silencing and was used as control to normalize H3K9 acetylation levels at the *L-PK* promoter ($n$ = 8 per group; *$P$ < 0.05). Data represent mean ± SEM.

1H). The increase in acetyl-CoA content as well as the increase in acetylation at both global level and specific genomic regions suggest that altered histone acetylation may contribute to changes in gene expression observed in liver of SIK2i mice.

*SIK2-mediated phosphorylation of p300 on Ser89 inhibits its HAT activity*. To determine the molecular mechanism by which SIK2 enhances fatty acid synthesis at the level of chromatin organization and transcription, we conducted a proteomic analysis to identify new SIK2-interacting proteins in hepatocytes and recovered the coactivator p300, known to play an important role in transcription. We confirmed the SIK2-p300 interaction in coimmunoprecipitation studies using epitope-tagged p300 and SIK2 constructs (Figure 2A). Analysis of the amino acid sequence of p300 led to identification of Ser89 as a consensus recognition phosphorylation motif for SIK2 in p300 (Figure 2B). Phosphorylation of p300 at Ser89 has been previously reported to regulate its transcriptional activity, although the underlying mechanism remains unclear (21, 26). In the current study, using an in vitro kinase assay, we demonstrated that SIK2 phosphorylates p300 only at Ser89, since SIK2, without affecting its capacity to interact with p300, was unable to phosphorylate p300 containing a point mutation at Ser89 to alanine (S89A p300) (Figure 2A). These results were confirmed using a phospho-specific Ser89 p300 antibody (Figure 2A). In vivo, in the fed state, p300 was phosphorylated on Ser89 in liver of USi mice, consistent with the upregulation of SIK2 activity by insulin during feeding (23) (Figure 2C). Interestingly, in liver of SIK2i mice, reduced amounts of Ser89-phosphorylated p300 were detected, indicating that p300 is probably a direct substrate of SIK2 in vivo (Figure 2C).

We next investigated whether phosphorylation at Ser89 of p300 by SIK2 affected its function. Expression constructs containing a Gal4 DNA-binding domain fused to either WT p300 (Gal4-WT-p300) or p300 containing a point mutation at Ser89 to alanine (Gal4-S89A-p300) were transfected in HepG2 cells (Figure 2D). Coexpression of SIK2 repressed Gal4-WT-p300 activity by 3-fold compared with control, while SIK2 had no effect on Gal4-S89A-p300 activity (Figure 2D). Interestingly, Gal4-S89A-p300 was more active than Gal4-WT-p300, suggesting that phosphorylation of p300 by SIK2 represses its transcriptional ability. In support of this hypothesis, staurosporine (STS, an inhibitor of SIK2 activity) treatment markedly reduced amounts of Ser89 p300 phosphorylation in cells overexpressing SIK2, and as a result, its transcriptional activity was increased (Figure 2E). To examine whether SIK2-mediated phosphorylation directly affected p300 function, we carried out p300 HAT assays using free core histones and p300 that was previously phosphorylated by SIK2 in HEK293T cells. We observed that the HAT activity of WT p300 was markedly reduced by SIK2-mediated Ser89 phosphorylation (Figure 2F). In contrast, SIK2 did not affect HAT activity of S89A p300, indicating that the repression of p300 HAT activity was specific to the phosphorylation at Ser89. Similar data were obtained when we used GST-CRTC2, a well-known substrate of p300 (21, 26), instead of free core histones as a HAT substrate, providing further evidence for a decreased p300 activity in the presence of SIK2 (Supplemental Figure 2A). This decrease in p300 HAT activity by SIK2 was specific, since SIK2 was unable to decrease the HAT activity of several major HAT proteins, such as CBP, PCAF, and GCN5, known to play an important role in the regulation of gene transcription (Supplemental Figure 2B). We also carried out functional p300 HAT assays in vivo (Figure 2G). The decrease in Ser89 p300 phosphorylation in liver of SIK2i mice (Figure 2C) was associated with a 2-fold increase in p300 HAT activity (Figure 2G). Therefore, our data suggest that the development of hepatic steatosis in liver of SIK2i mice could be linked to increased p300 activity, leading to enhanced glycolytic and lipogenic gene transcription through histone and non-histone protein acetylation.

*p300 and ChREBP co-occupy the L-PK gene promoter in a glucose-dependent manner*. To further address the role of p300, we next examined whether p300 directly interacted with the *L-PK* promoter in cultured hepatocytes (Figure 3). ChIP assays revealed that the recruitment of p300, ChREBP, and RNA polymerase II, in addition to the acetylation levels of histones H3K9 and H4K8, at the *L-PK* promoter were markedly increased after glucose stimulation (Figure 3A and Supplemental Figure 3, A–C). Together, these events led to increased ChoRE-luciferase reporter activity (ChoRE-luc: reporter containing only ChREBP-binding sites) (Figure 3B) as well as *L-PK* and *Fas* gene expression (Figure 3C). Importantly, inhibiting p300 expression decreased the glucose-stimulated association of ChREBP with the *L-PK* promoter, demonstrating that p300 is necessary for the binding of ChREBP to DNA (Figure 3, A and D). Interestingly, p300 recruitment to the *L-PK* promoter was also ChREBP-dependent (Supplemental Figure 4). Indeed, in ChREBP-deficient hepatocytes (Supplemental Figure 4A), p300 and RNA polymerase II recruitment as well as acetylated histones H3K9 and H4K8 at the ChoRE-containing region of the *L-PK* promoter were not detected, leading to the inhibition of ChoRE-luc activity and glycolytic and lipogenic gene expression (Supplemental Figure 4, B–D). Taken together, our observations show that p300 and ChREBP are required for each other's ability to bind to the *L-PK* promoter. To further determine whether p300 and ChREBP are simultaneously associated to the *L-PK* promoter in glucose-treated hepatocytes, chromatin immunoprecipitated with ChREBP antibody was re-precipitated with p300 antibodies in a sequence-ChIP (seq-ChiP) experiment. *L-PK* promoter sequences were detected in hepatocytes re-precipitated with p300 antibodies (Supplemental Figure 3E). These results suggest that p300 and ChREBP are simultaneously associated and co-occupy the *L-PK* promoter in a glucose-dependent manner. This ChREBP-p300 interaction was confirmed in coimmunoprecipitation studies using epitope-tagged p300 and

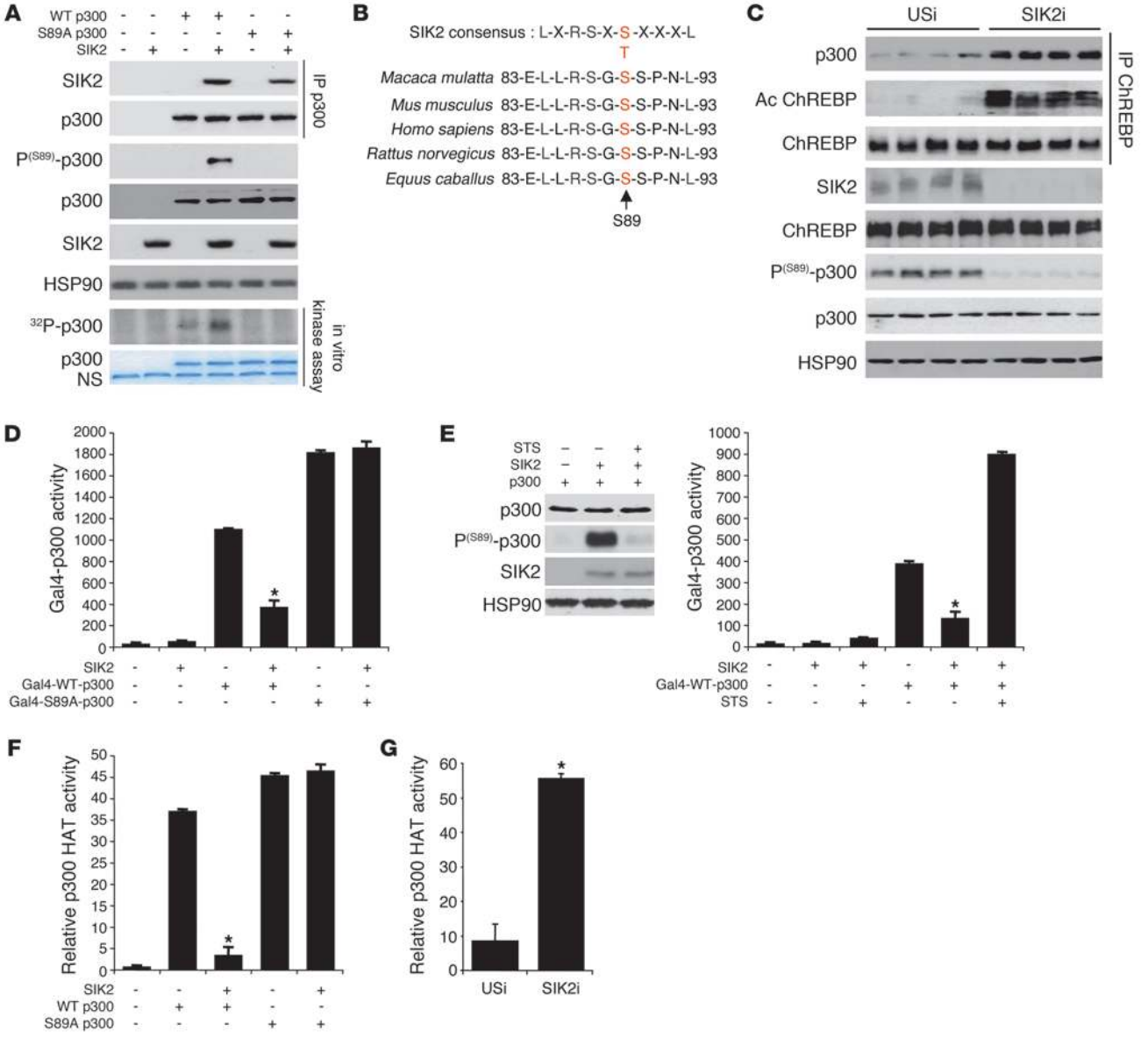


**Figure 2**

SIK2 promotes p300 Ser89 phosphorylation and inhibits p300 activity. (**A**) Top 2 panels: Coimmunoprecipitation assay from HepG2 cells using epitope-tagged p300 and SIK2 proteins. The amount of SIK2 recovered from IPs of p300 is shown. Middle 4 panels: Western blot analysis of p300 with specific anti–phospho-Ser89 antiserum after phosphorylation by SIK2. Bottom 2 panels: Autoradiograph showing phosphorylation of p300 at Ser89 by SIK2 in an in vitro kinase assay. Data are representative of 3 independent experiments. NS, nonspecific. (**B**) p300 phosphorylation site at Ser89 by SIK2 is conserved across eukaryotic species. (**C**) Western blot analysis of phosphorylated Ser89 p300 and acetylated ChREBP levels in liver of USi and SIK2i mice ($n$ = 8 per group). (**D**) Measurement of Gal4-WT and S89A p300 activity in HepG2 cells overexpressing SIK2. Data are the average of 3 independent experiments (mean ± SEM; *$P$ < 0.05). (**E**) Left: Western blot analysis of p300 Ser89 phosphorylation after STS treatment in HepG2 cells. Data are representative of 3 independent experiments. Right: Measurement of UAS-luciferase activity in HepG2 cells overexpressing Gal4-WT-p300 with SIK2 after STS treatment. Data are the average of 3 independent experiments (mean ± SEM; *$P$ < 0.05). (**F**) Inhibition of p300 HAT activity via phosphorylation at Ser89 by SIK2. WT or S89A p300 were overexpressed in HepG2 cells with or without a SIK2 expression vector. p300 was then immunoprecipitated and used for HAT assays on core histone proteins. Data are the average of 3 independent experiments (mean ± SEM; *$P$ < 0.05). (**G**) p300 HAT activity in liver of USi and SIK2i mice ($n$ = 8 per group; data represent mean ± SEM; *$P$ < 0.01).

ChREBP protein (Supplemental Figure 3G). Because the glucose-mediated recruitment of RNA polymerase II to the *L-PK* promoter was dependent upon p300 and ChREBP, we next examined whether RNA polymerase II was also present on the promoter as part of the p300/ChREBP complex. A seq-ChIP experiment with p300 revealed a 2.8-fold increase in RNA polymerase II seq-ChIP signal at 25 mM glucose (Supplemental Figure 3F). Similar results were found using a ChREBP antibody for the first round of immunoprecipitation

(data not shown). From the cumulative findings shown in Figure 3 and Supplemental Figure 3, we conclude that RNA polymerase II is recruited to the *L-PK* gene promoter in a glucose-dependent manner, as part of a p300/ChREBP complex, which is required for maximal transcription by glucose.

*p300 associates and regulates ChREBP transcriptional activity by acetylation*. To date, the involvement of p300 via its HAT activity in the glucose-mediated regulation of ChREBP activity by acetylation has not been demonstrated to our knowledge. To examine whether ChREBP can be acetylated, we incubated HepG2 cells overexpressing epitope-tagged ChREBP with or without a p300 expression vector, in the presence of [$^3$H]acetate for 1 hour. As shown in Figure 3E, ChREBP is an acetylated protein, and p300 overexpression enhanced this acetylation. Furthermore, coincubation of HepG2 cells with Lys-CoA-TAT (a cell-permeable p300 HAT inhibitor) abolished the acetylation of ChREBP by p300 (Figure 3E). These results were confirmed by Western blotting of ChREBP immunoprecipitated with antiserum that recognized acetylated lysine, which showed that acetylated ChREBP levels were elevated in cells overexpressing p300 (Supplemental Figure 3G). In addition, acetylation levels of ChREBP were increased in liver of SIK2i mice, concomitantly or concurrent with upregulation of p300 HAT activity (Figure 2, C and G). In a seq-ChIP experiment, we demonstrated that ChREBP was highly acetylated on the *L-PK* promoter in response to glucose stimulation and found that p300 overexpression increased its acetylation (Figure 3D and Supplemental Figure 3H). In addition, we found that ChREBP was only acetylated in the nucleus of hepatocytes upon glucose stimulation, when it associated with p300 (data not shown). Then, to determine whether the HAT activity of p300 is important for the regulation of ChREBP function by acetylation, we examined the effect of p300 overexpression on Gal4-ChREBP transactivation potency in HepG2 cells. Overexpression of p300 significantly enhanced Gal4-ChREBP transactivation activity, and this effect was abolished by coincubation with Lys-CoA-TAT or by overexpression of a catalytically inactive p300 mutant in which the HAT domain was deleted (Figure 3E and Supplemental Figure 4E). To further determine the functional specificity of p300 HAT activity in ChREBP function, we examined the recruitment of p300, CBP, GCN5, and PCAF to the *L-PK* promoter by ChiP studies in hepatocytes. Although the recruitment of CBP on the *L-PK* promoter was slightly increased, there was no association of GCN5 and PCAF to the *L-PK* promoter in response to glucose stimulation (Supplemental Figure 5B). Then, to test whether these HATs were able to acetylate and regulate ChREBP activity, we performed in vitro acetylation studies. ChREBP was acetylated by p300 and to a lesser extent by CBP, but not by GCN5 or PCAF (Supplemental Figure 5A). However, as expected, histones were robustly acetylated by all of these acetylases (Supplemental Figure 5A). In contrast to p300 overexpression, ChREBP transactivation potency (i.e., ChREBP occupancy to the *L-PK* promoter, Gal4-ChREBP, and ChoRE-luc activities) was not increased upon GCN5 and PCAF overexpression and only modestly increased by CBP. These results suggest that p300 and to a lesser extent CBP, but not GCN5 and PCAF, are directly involved in the glucose-dependent induction of ChREBP by acetylation, suggesting functional specificity of acetylases in the regulation of ChREBP transcriptional activity.

*p300-mediated acetylation of ChREBP at Lys672 increases its DNA binding activity*. To further define the functional role of ChREBP acetylation, we identified acetylated lysine (K) residues using tandem mass spectrometry (MS/MS). Flag-tagged ChREBP was expressed in HEK293T cells and was acetylated by p300 (Figure 4 and Supplemental Figure 6). The MS/MS analysis revealed that K658, K672, and K678 located in the DNA-binding domain of ChREBP were the major sites acetylated by p300 (Figure 4A). The total coverage of peptides for all the ChREBP MS/MS analysis is depicted in Supplemental Figure 6A and was about 46% when trypsin was used for digestion. To confirm these results, we cotransfected cells with plasmids coding for p300 and either WT ChREBP or one of the acetylation-defective ChREBP mutants (ChREBP K658R, K672R, and K678R). ChREBP acetylation levels were significantly reduced in K658R, K672R, and K678R mutants compared with WT ChREBP, indicating that these particular lysines are targeted by p300 for acetylation in vitro (Figure 4B and Supplemental Figure 6B). It is important to note that K658R, K672R, and K678R mutations in ChREBP did not change the capacity of p300 to interact with ChREBP (Figure 4B). Next, we determined whether acetylation of ChREBP affected its transactivation ability by analyzing ChoRE-luc activity in the presence of the K658R, K672R, and K678R mutants. The K672R mutant was the only one to drastically decrease ChREBP activity stimulated by p300 compared with WT (Figure 4A). This result indicates that ChREBP transactivation activity is increased when ChREBP is acetylated by p300 at K672.

Acetylation of transcription factors often alters their activity dependent on the functional domains that are modified (27). In the case of ChREBP, Lys672, which has a high impact on ChREBP transcriptional activity in response to p300, is located within the basic region of the DNA-biding domain (Figure 4A) and is adjacent to two arginine (R) residues (R673 and R674) previously described to be important to support the glucose response by ChREBP (28). Indeed, mutation of R673 and R674, respectively, to alanine and glutamine totally abolished the binding of ChREBP to its target gene promoter and inhibited its transcriptional activity. This ChREBP mutant works as a dominant negative form (ChREBP DN) in hepatocytes (28). Given that K672 is localized contiguously to these two arginines, we checked whether this specific acetylation site could influence ChREBP DNA-binding activity. To assess this possibility, we performed ChIP analysis on the *L-PK* promoter using ChREBP DN as a negative control (Figure 4, C–E). As expected, p300 overexpression, by increasing ChREBP acetylation levels, enhanced WT ChREBP occupancy to the *L-PK* promoter and consequently potentiated the induction of *L-PK* gene expression. In contrast, despite the fact ChREBP DN was normally acetylated by p300, there was no recruitment of this mutant to the *L-PK* promoter in response to p300 overexpression. As a consequence, ChREBP DN was unable to induce the expression of *L-PK* in response to p300 overexpression. Interestingly, the amount of DNA-bound K672R ChREBP mutant was not enhanced by p300 overexpression and correlated with decreased ChREBP acetylation levels (Figure 4, C–E). Under this condition, K672R ChREBP was unable to induce *L-PK* expression when p300 was overexpressed. However, it is interesting to note that DN or K672R ChREBP is still able to interact with Mlx after p300 overexpression, confirming that the lack of LPK expression is the result of a decreased recruitment of these mutants to the ChoRE of the *L-PK* promoter rather than a modification in the heterodimer formation at the promoter. To further assess the transcriptional activities of K672R and DN ChREBP mutants, we used a different functional assay that allowed us to measure the activity of these mutants relative to WT ChREBP (Supplemental Figure 6C). In

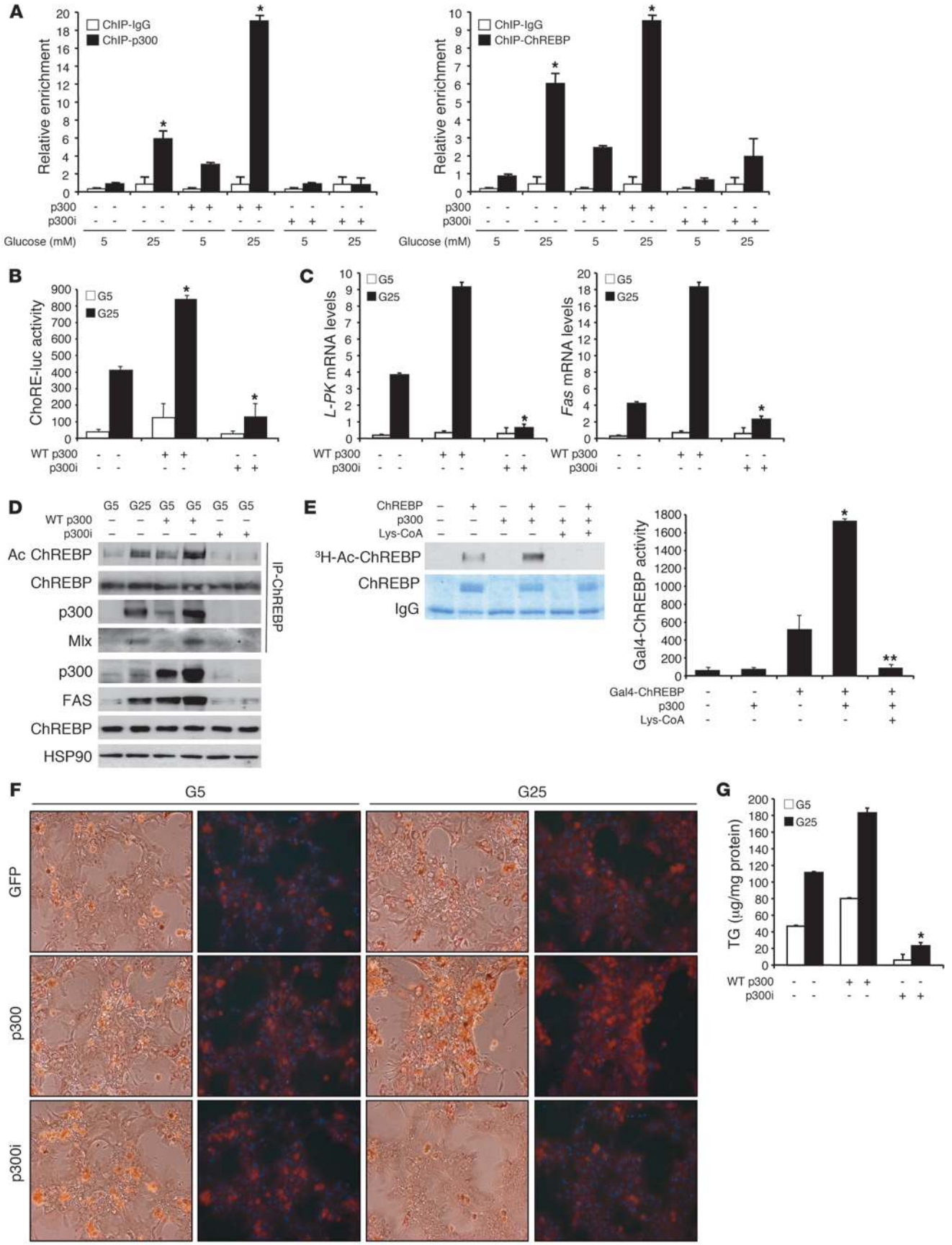
A
ChIP-IgG
ChIP-p300
Relative enrichment
p300
p300i
Glucose (mM)
ChIP-IgG
ChIP-ChREBP
B
ChoRE-luc activity
G5
G25
WT p300
C
L-PK mRNA levels
Fas mRNA levels
D
Ac ChREBP
ChREBP
p300
Mlx
IP-ChREBP
FAS
HSP90
E
ChREBP
Lys-CoA
3H-Ac-ChREBP
IgG
Gal4-ChREBP activity
Gal4-ChREBP
F
GFP
G
TG (μg/mg protein)

**Figure 3**
p300 promotes fatty acid synthesis through the regulation of ChREBP activity by acetylation. Effects of p300 overexpression or p300 silencing on glucose and lipid metabolism in hepatocytes incubated in the presence of insulin (100 nM) and either 5 or 25 mM glucose (G5 or G25) for 18 hours. (**A**) ChIP assay showing p300 and ChREBP recruitment to the *L-PK* promoter following treatment with glucose. Data are the average of 3 independent experiments (mean ± SEM; $^*P < 0.05$). (**B**) ChoRE-luc reporter activity in HepG2 cells. Data are the average of 5 independent experiments (mean ± SEM; $^*P < 0.05$). (**C**) Relative expression of genes encoding LPK and FAS measured by quantitative PCR (data represent mean ± SEM of 3 independent experiments; $^*P < 0.01$). (**D**) Western blot analysis of p300 and acetylated ChREBP levels. Data are representative of 3 independent experiments. (**E**) Left: HepG2 cells overexpressing epitope-tagged p300 and ChREBP proteins were incubated 1 hour in the presence of [$^3$H]acetate. FLAG-ChREBP was immunoprecipitated. An autoradiogram of $^3$H-acetylated-FLAG-ChREBP is shown. Data are representative of 3 independent experiments. Right: ChREBP transcriptional activity was measured in HepG2 cells overexpressing p300 and a Gal4-ChREBP fusion protein. Transcriptional activity was calculated from a ratio of luciferase to β-gal activities. Experiments were carried out in triplicate. Data represent mean ± SEM; $^*P < 0.01$. (**F**) Oil red O staining of neutral lipids. Original magnification, ×200. Data are representative of 3 independent experiments. (**G**) TG concentrations. Data are representative of 3 independent experiments. Data represent mean ± SEM; $^*P < 0.01$.

this competition assay (28), a constant amount of WT ChREBP was inhibited by transduction of cells with either ChREBP DN or K672R mutants. Interestingly, overexpressing ChREBP DN or K672R inhibited in a dose-dependent manner the capacity of WT ChREBP to induce ChoRE-luc activity under both basal and p300 overexpression conditions. Finally, we tested the role of K672 acetylation in the glucose-dependent regulation of ChREBP transcriptional activity in hepatocytes (Figure 4, F–I). Acetylation of the ChREBP K672R mutant and its recruitment to the *L-PK* promoter were significantly reduced in response to glucose treatment compared with WT ChREBP (Figure 4F and Supplemental Figure 6D). As a consequence, *L-PK* expression and TG synthesis were reduced (Figure 4, H and I). Taken together, our results demonstrate that the p300-mediated acetylation of ChREBP within its DNA-binding domain at K672 promotes its recruitment to the ChoRE of the *L-PK* promoter.

*p300 is a rate-limiting transcriptional coactivator in the regulation of fatty acid synthesis in hepatocytes*. Since p300 is recruited to the *L-PK* promoter in a glucose-dependent manner and plays an important role in the regulation of ChREBP activity by acetylation, the function of p300 in the regulation of glycolytic and lipogenic gene expression and fatty acid synthesis was analyzed by testing the effects of p300 overexpression or inhibition in cultured hepatocytes. Overexpression of p300 increased whereas its downregulation significantly decreased the amount of acetylated ChREBP (Figure 3D and Supplemental Figure 3H). As a consequence, p300 silencing resulted in a substantial decrease in both LPK and FAS expression in response to glucose, whereas p300 overexpression enhanced their expression (Figure 3C). In functional reporter assays, overexpression of p300 significantly increased ChREBP transactivation (increase in ChoRE-luc reporter activity), whereas inhibition of p300 expression prevented this effect (Figure 3B). Interestingly, inhibition of p300 expression in hepatocytes led to decreased fatty acid and TG synthesis (Figure 3, F and G), whereas p300 overexpression increases their cellular content. Addition of Lys-CoA or curcumin (a specific p300 inhibitor) to cultured hepatocytes confirmed these results (Supplemental Figure 7), by reducing the amount of acetylated ChREBP (Supplemental Figure 7, A and E), ChoRE-luc activity (Supplemental Figure 7, C and G), expression of glycolytic and lipogenic genes and TG concentrations in response to glucose and insulin (Supplemental Figure 7, B, D, F, and H). To our knowledge, our study is the first to report the absolute requirement of p300 in the ChREBP-mediated glucose effect on glycolytic and lipogenic genes to promote fatty acid synthesis.

*p300 mediates the SIK2-elicited inhibition of ChREBP-dependent induction of lipogenesis in hepatocytes*. We further tested the possibility that SIK2-mediated repression of lipogenesis was directly linked to the inhibition of p300 HAT activity and consequently to the inhibition of ChREBP activity. As shown in Figure 5, A and B, inhibition of SIK2 expression in cultured hepatocytes decreased p300 S89 phosphorylation, enhanced p300 HAT activity, and increased the recruitment of ChREBP to the *L-PK* promoter (Figure 5C and Supplemental Figure 8A). As a consequence, p300 HAT activation enhanced the acetylation of H3K9 and H4K8 and ChREBP and increased ChoRE-luc activity in response to glucose stimulation (Figure 5, A and D, and Supplemental Figure 8, B and C). However, coinhibition of p300 expression with SIK2 in hepatocytes successfully counteracted the stimulatory effect observed in SIK2i-treated cells, by decreasing ChREBP acetylation and transcriptional activity, as demonstrated by decreased ChoRE-luc activity, glycolytic and lipogenic gene expression, and fatty acid synthesis (Figure 5, A, C, D, and E, and Supplemental Figure 8, B, D, and E). Finally, to confirm these results, we cotransfected HepG2 cells with either WT or S89A p300 in the presence or absence of SIK2 in a Gal4-ChREBP reporter assay. As expected, both the WT and S89A mutant of p300 enhanced Gal4-ChREBP and ChoRE-luc activity by increasing ChREBP acetylation levels (Figure 5, G–I). Coexpression of SIK2 repressed WT p300–mediated induction of Gal4-ChREBP and ChoRE-luc activity by 3-fold (Figure 5, H and I). However, the effect of SIK2 overexpression on Gal4-ChREBP reporter activity was abolished in cells cotransfected with the S89A p300 mutant. These results strongly correlate with the fact that SIK2 is unable to inhibit S89A p300 HAT activity by phosphorylation to prevent ChREBP activation by acetylation (Figure 5G). Finally, reduced hepatic TG levels caused by SIK2 overexpression were restored to normal levels when the S89A mutant of p300 was coexpressed (Figure 5J). These results demonstrate that the phosphorylation at Ser89 and subsequent inhibition of p300 activity were the key events leading to the downregulation of ChREBP activity in SIK2-overexpressing hepatocytes.

*Dysregulation of p300 activity in vivo leads to the development of hepatic steatosis, inflammation, and insulin resistance*. Together, our data showed so far that p300 may participate in the development of hepatic steatosis in liver of SIK2i mice, particularly by enhancing glycolytic and lipogenic gene transcription via the modulation of ChREBP activity by acetylation. These results suggest that decreased SIK2 activity in states of insulin resistance could be responsible for the upregulation of fatty acid synthesis, leading to the development of hepatic steatosis. In the present study, we found that SIK2 kinase activity, which is physiologically activated by insulin (23) and inhibited by glucagon (29), was downregulated in liver of fed *ob/ob* mice or mice fed on a high-fat diet (HFD) for 4 months (Supplemental Figure 9A). These two mouse models of obesity and type 2 diabetes showed severe hepatic insulin resistance as demonstrated by fasting hyperglycemia (82.5 ± 6.4 for

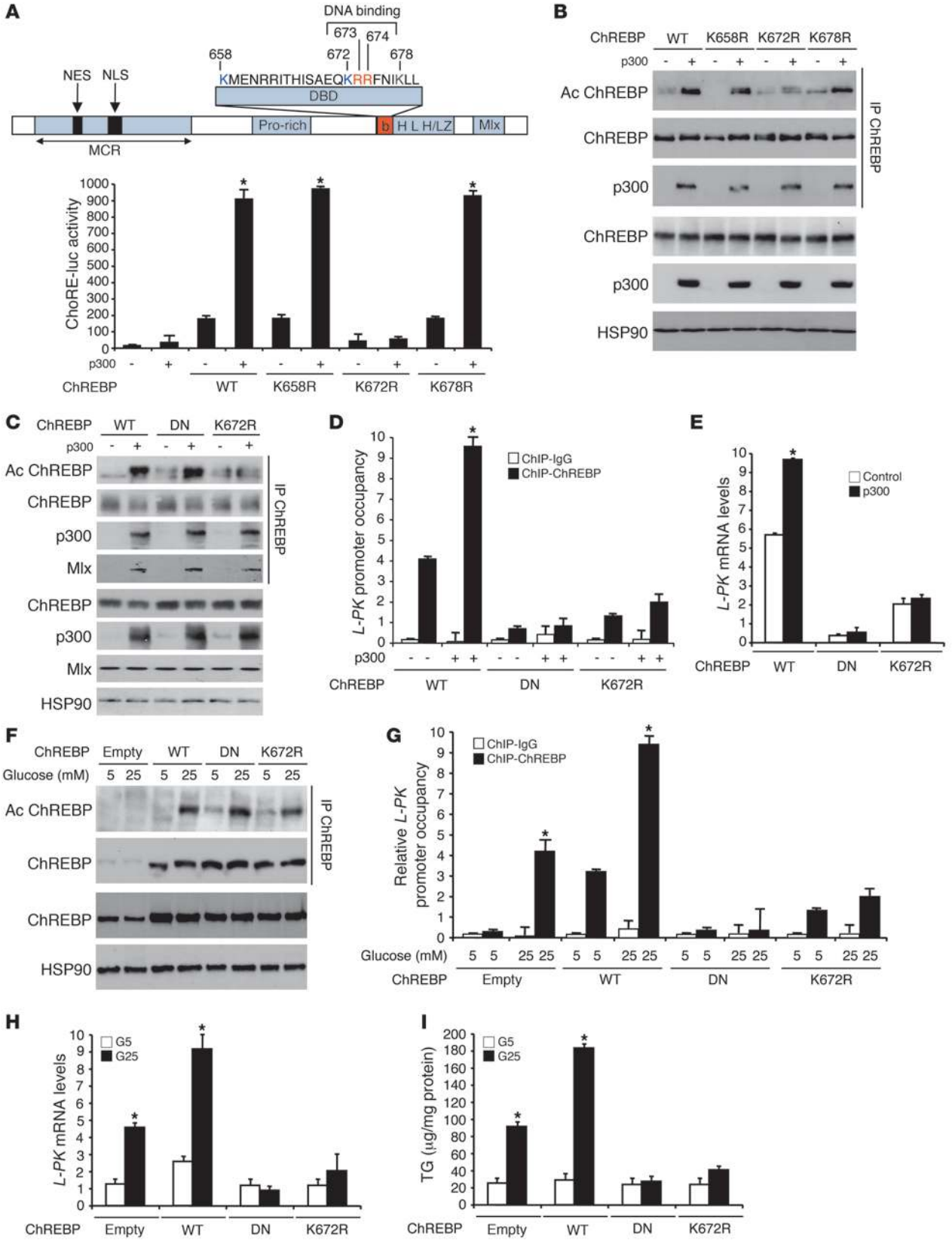
A
DNA binding
673 674
658
672
678
KMENRRITHISAEQKRRFNIKLL
NES NLS
DBD
Pro-rich
b
H L H/LZ
Mlx
MCR
ChoRE-luc activity
p300
ChREBP
WT
K658R
K672R
K678R
B
ChREBP
WT
K658R
K672R
K678R
p300
Ac ChREBP
ChREBP
p300
ChREBP
p300
HSP90
IP ChREBP
C
ChREBP
WT
DN
K672R
p300
Ac ChREBP
ChREBP
p300
Mlx
ChREBP
p300
Mlx
HSP90
IP ChREBP
D
L-PK promoter occupancy
ChIP-IgG
ChIP-ChREBP
p300
ChREBP
WT
DN
K672R
E
L-PK mRNA levels
Control
p300
ChREBP
WT
DN
K672R
F
ChREBP
Empty
WT
DN
K672R
Glucose (mM)
5 25 5 25 5 25 5 25
Ac ChREBP
ChREBP
ChREBP
HSP90
IP ChREBP
G
Relative L-PK promoter occupancy
ChIP-IgG
ChIP-ChREBP
Glucose (mM)
5 5 25 25 5 5 25 25 5 5 25 25 5 5 25 25
ChREBP
Empty
WT
DN
K672R
H
L-PK mRNA levels
G5
G25
ChREBP
Empty
WT
DN
K672R
I
TG (μg/mg protein)
G5
G25
ChREBP
Empty
WT
DN
K672R

**Figure 4**
Acetylation of ChREBP at Lys672 increases its binding to the DNA. (**A**) Top: Localization of ChREBP acetylation sites in its DNA-binding domain. Bottom: Effect of single point mutation of ChREBP acetylation sites on ChoRE-luc reporter activity in HepG2 cells overexpressing p300. (**B**) HepG2 cells transfected with p300 and with acetylation-deficient FLAG-ChREBP mutants. FLAG-ChREBP was immunoprecipitated, and acetylated ChREBP was detected by Western blot. (**C**) Acetylation levels of WT, DN, or K672R ChREBP by p300 in HepG2 cells. Mlk (Max-like protein X) is a ChREBP heteropartner required for ChREBP transcriptional activity in hepatocytes. (**D**) ChIP assay showing the effect of K672R mutation on ChREBP recruitment to the *L-PK* promoter following p300 overexpression in HepG2 cells. (**E**) Effect of K672R ChREBP mutant on *L-PK* expression in HepG2 cells overexpressing p300. (**F**) Acetylation levels of WT, DN, or K672R ChREBP in hepatocytes incubated with insulin and 5 or 25 mM glucose. (**G**) ChIP assay showing the effect of K672R mutation on ChREBP recruitment to the *L-PK* promoter in hepatocytes incubated with insulin and either 5 or 25 mM glucose. (**H**) Effect of K672R ChREBP mutant on LPK expression in hepatocytes incubated with insulin and either 5 or 25 mM glucose. (**I**) Effect of K672R ChREBP mutant on TG synthesis in hepatocytes incubated with insulin and either 5 or 25 mM glucose. In this figure, data are the average of 3 independent experiments (mean ± SEM; $^*P < 0.01$).

chow diet vs. 145.4 ± 3.12 mg/dl for HFD, $P < 0.05$; and 88.4 ± 3.4 for *ob/+* vs. 245.8 ± 8.5 mg/dl for *ob/ob*, $P < 0.02$), hyperinsulinemia (Supplemental Figure 9B), and the inability of insulin to stimulate Akt phosphorylation (Supplemental Figure 9, C and D). In the fed state, *ob/ob* and HFD-fed mice also displayed increased plasma glucagon concentrations and liver PKA activity when compared with *ob/+* and chow diet–fed mice, respectively (Supplemental Figure 9, B and E). Together, the data indicate that decreased hepatic insulin signaling and enhanced PKA activity inhibited SIK2 kinase activity in these two models. Since decreased SIK2 activity is associated with reduced p300 Ser89 phosphorylation (Supplemental Figure 9, C and D), p300 HAT activity was enhanced in these mouse models, increasing ChREBP acetylation levels and lipogenesis when compared with control mice (Supplemental Figure 9, C, D, and F). Overall, our results demonstrate that enhanced p300 HAT activity in states of obesity and insulin resistance, as a result of decreased SIK2 kinase activity, is correlated with the development of hepatic steatosis. Thus, we finally tested whether dysregulation of p300 activity in vivo could indeed lead to the development of fatty liver. Adenovirus-mediated overexpression of p300 led to severe hepatosteatosis (Figure 6A), with marked accumulation of large lipid droplets and higher TG and NEFA concentrations compared with GFP-overexpressing mice (Figure 6, A and D, and Supplemental Figure 10A). p300 overexpression enhanced both its HAT activity and recruitment to the *L-PK* promoter (Figure 6C and Supplemental Figure 10B). As a consequence, p300 overexpression increased H3K9 and ChREBP acetylation levels (Figure 6, B and G), increased ChREBP occupancy to the *L-PK* promoter (Figure 6G), and enhanced *L-PK*, *Acl*, *Acc*, and *Fas* gene expression, with no change in mRNA expression levels of either *ChREBP* or *SREBP-1c* (Figure 6E and Supplemental Figure 10C). By enhancing the induction of ACL and lipogenesis, p300 overexpression increased the synthesis of acetyl-CoA (Figure 6F and Supplemental Figure 10C), which is used to acetylate histone H3K9 and ChREBP to promote fatty acid synthesis and development of hepatic steatosis. However, increased acetyl-CoA content only affected a select set of substrates, since the acetylation of tubulin was unchanged when p300 was overexpressed (Supplemental Figure 10B). Importantly, all of these effects were reversed by SIK2 co-overexpression. Indeed, SIK2- and p300-overexpressing mice were almost entirely protected from nonalcoholic fatty liver disease (NAFLD), showing lipid droplets that were smaller in number and diameter and a reduction in both TG and NEFA concentrations (Figure 6, A and D, and Supplemental Figure 10A). SIK2 overexpression inhibited p300 HAT activity by increasing its Ser89 phosphorylation (Figure 6, B and C) and decreased its recruitment to the *L-PK* promoter (Supplemental Figure 10B). In agreement with the observation that SIK2 protects from p300-mediated hepatic steatosis, we found that SIK2 and p300 co-overexpressing mice presented lower acetyl-CoA concentrations (Figure 6F), decreased H3K9 and ChREBP acetylation levels (Figure 6, B and G), and, as a consequence, reduced glycolytic and lipogenic gene expression (Figure 6E and Supplemental Figure 10C). Together, these data demonstrated that increased SIK2 activity leads to the significant improvement of hepatic steatosis and dyslipidemia induced by p300.

Consistent with the development of hepatic steatosis, p300 overexpression increased plasma glucose, insulin, TG, and NEFA concentrations, whereas SIK2 co-overexpression restored these parameters to GFP control levels (Figure 6, D and E, Figure 7A, and Supplemental Figure 10A). Based on reports showing that liver and peripheral insulin resistance can also be a direct consequence of NAFLD (reviewed in ref. 5), we next examined whether glucose tolerance and insulin sensitivity differed between GFP- and p300-overexpressing mice (Figure 7A). Consistent with the development of hepatic steatosis, p300-overexpressing mice became largely glucose intolerant and insulin-resistant compared with GFP-overexpressing mice (Figure 7A). In particular, p300 overexpression led to the development of liver insulin resistance characterized by decreased Akt phosphorylation (Figure 6B) and reduced glycogen content in the fed state (Supplemental Figure 10F). As a result of the state of insulin resistance, Ser171 CRTC2 phosphorylation decreased (Figure 6B), and *Pepck* and *G6Pase* gene expression was upregulated in livers of p300-overexpressing mice, leading to the development of postprandial hyperglycemia (Figure 7, A and B). However, SIK2 overexpression, by preventing fat accumulation, totally protected mice from the effects of p300 overexpression. Area under the curve of oral glucose tolerance and insulin tolerance tests (OGTT and ITT) revealed an improvement in both glucose tolerance and insulin sensitivity in mice co-overexpressing SIK2 and p300 (Figure 7A). SIK2 overexpression increased phosphorylation of CRTC2, and as a result expression of *Pepck* and *G6Pase* was strongly reduced, corroborating the improvement of hepatic insulin sensitivity and glucose tolerance (Figure 6B and Figure 7, A and B).

Since hepatic steatosis is generally associated with inflammation, known markers of inflammatory response were measured in p300-overexpressing mice. Circulating levels of IL-6, resistin, and TNF-α, regulated by NF-κB, itself activated by dietary lipids (30), were significantly enhanced in p300-overexpressing mice (Supplemental Figure 10D). In comparison, SIK2-overexpressing mice exhibited significantly lower levels of inflammatory markers. Interestingly, p300 was previously described to enhance NF-κB activity (31) and to increase the secretion of IL-6 (32). To evaluate whether NF-κB was downregulated by SIK2-mediated inhibition of p300 function, we examined NF-κB activity by using a luciferase reporter gene assay under the transcriptional control of NF-κB

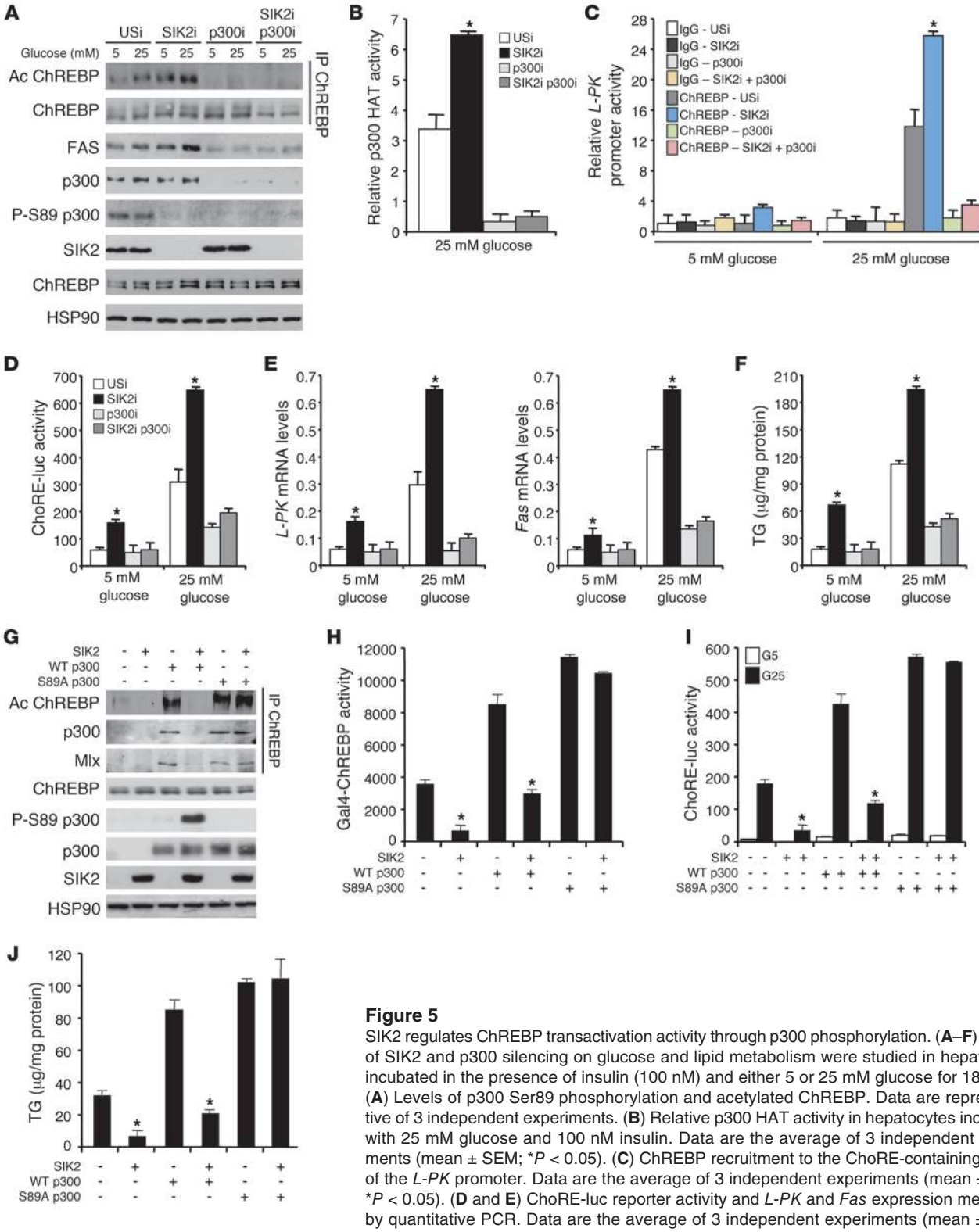


**Figure 5**

SIK2 regulates ChREBP transactivation activity through p300 phosphorylation. (**A**–**F**) Effects of SIK2 and p300 silencing on glucose and lipid metabolism were studied in hepatocytes incubated in the presence of insulin (100 nM) and either 5 or 25 mM glucose for 18 hours. (**A**) Levels of p300 Ser89 phosphorylation and acetylated ChREBP. Data are representative of 3 independent experiments. (**B**) Relative p300 HAT activity in hepatocytes incubated with 25 mM glucose and 100 nM insulin. Data are the average of 3 independent experiments (mean ± SEM; *$P < 0.05$). (**C**) ChREBP recruitment to the ChoRE-containing region of the *L-PK* promoter. Data are the average of 3 independent experiments (mean ± SEM; *$P < 0.05$). (**D** and **E**) ChoRE-luc reporter activity and *L-PK* and *Fas* expression measured by quantitative PCR. Data are the average of 3 independent experiments (mean ± SEM; *$P < 0.05$). (**F**) Hepatic TG concentrations. Data are representative of 3 independent experiments (mean ± SEM; *$P < 0.01$). (**G**–**I**) HepG2 cells were transfected with either WT or S89A p300 expression vector with or without SIK2. (**G**) ChREBP acetylation levels. The amount of total ChREBP and p300 is shown. Data are representative of 3 independent experiments. (**H** and **I**) Gal4-ChREBP transactivation and ChoRE-luc activities. Data are representative of 3 independent experiments (mean ± SEM; *$P < 0.05$). (**J**) TG content. Data are representative of 3 independent experiments (mean ± SEM; *$P < 0.05$).

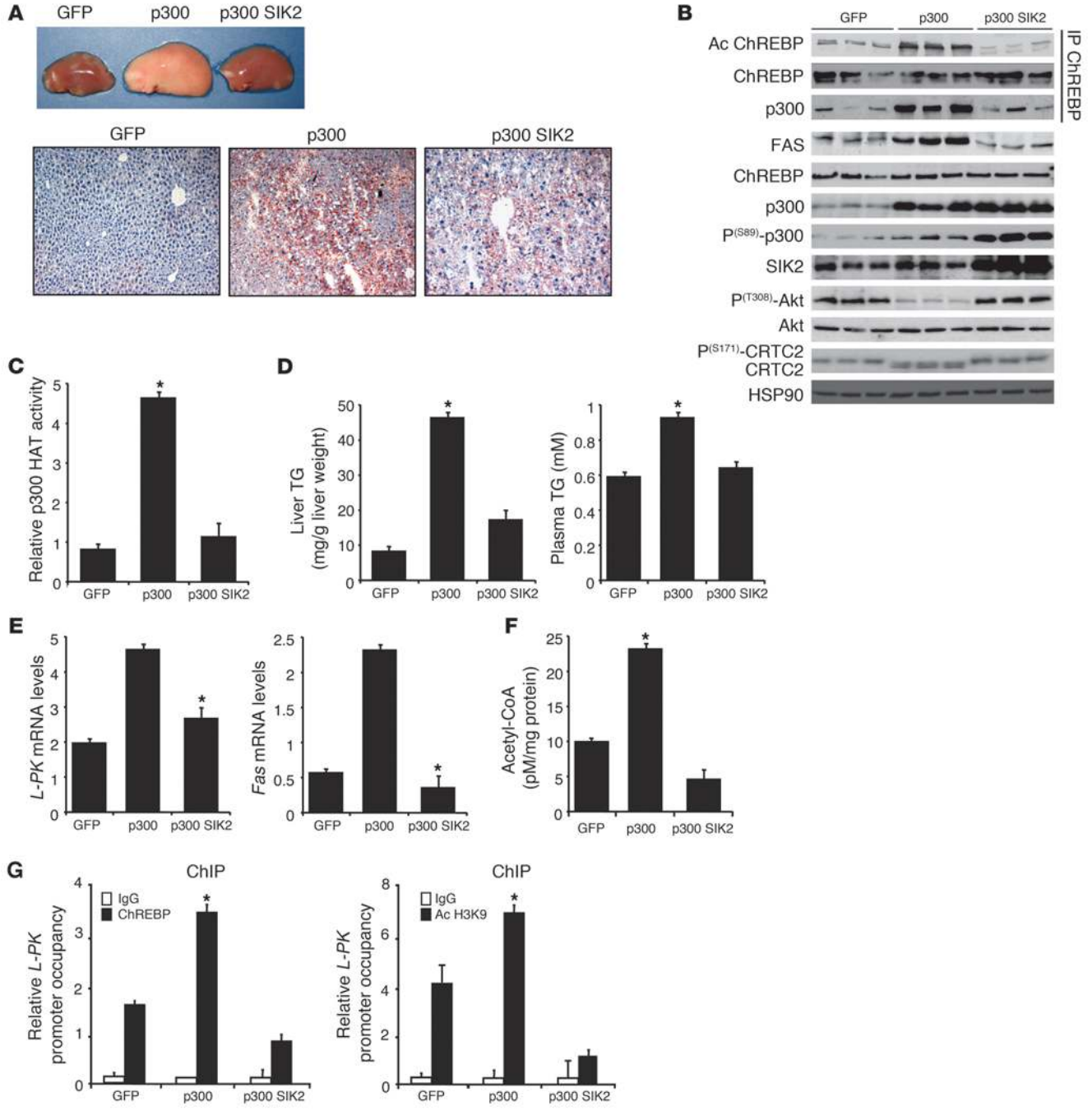


**Figure 6**

p300 overexpression impairs lipid homeostasis and leads to hepatic steatosis. Mice were injected with either p300 and/or SIK2 overexpressing adenovirus and studied 7 days later in the fed state. (**A**) p300-overexpressing mice develop hepatic steatosis as shown by increased liver size and oil red O staining of liver sections. Original magnification, ×200 ($n$ = 6 per group). (**B**) Western blot analysis of p300 and SIK2 protein content, acetylated ChREBP levels, and Akt phosphorylation on Thr308 ($n$ = 6 per group). (**C**) Liver relative p300 HAT activity ($n$ = 6 per group; *$P$ < 0.01). (**D**) Total liver and plasma TG levels ($n$ = 6 per group; *$P$ < 0.01). (**E**) Relative *L-PK* and *Fas* gene expression ($n$ = 6 per group; data represent mean ± SEM; *$P$ < 0.01). (**F**) Acetyl-CoA concentrations ($n$ = 6 per group; *$P$ < 0.01). (**G**) ChREBP recruitment and levels of acetylated H3K9 on the *L-PK* promoter measured by ChIP studies ($n$ = 8 per group; *$P$ < 0.05).

response elements (Figure 7C). Both WT and S89A p300 overexpression enhanced IL-6– (data not shown) and TNF-α–mediated activation of NF-κB in HepG2 cells (Figure 7C). In contrast, the TNF-α– and IL-6–mediated stimulation of NF-κB was lower in HepG2 cells overexpressing SIK2 and WT p300 but not in HepG2 cells coexpressing SIK2 and S89A p300 (Figure 7C). In addition, the amount of transaminases ALAT and ASAT was decreased in mice co-overexpressing SIK2 and p300 (Supplemental Figure

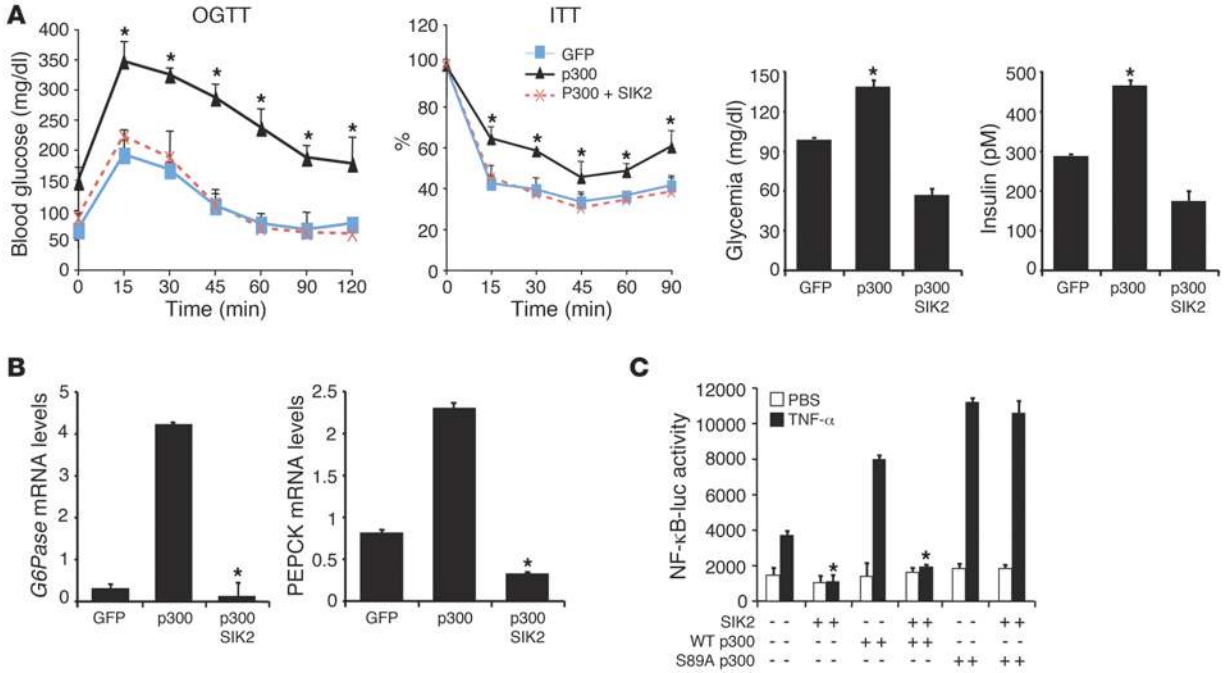


**Figure 7**

p300 overexpression impairs liver glucose homeostasis and leads to the development of glucose intolerance and insulin resistence. Mice were injected with p300- and/or SIK2-overexpressing adenovirus and studied 7 days later in the fed sate. (**A**) Left: OGTT and ITT. Right: Postprandial blood glucose and insulin concentrations ($n = 6$ per group; $^*P < 0.01$). (**B**) Relative *Pepck* and *G6Pase* gene expression ($n = 6$ per group; $^*P < 0.01$). (**C**) NF-κB–luc reporter gene assay. HepG2 cells were transfected with a NF-κB–luc reporter vector and stimulated with 10 ng/ml TNF-α. Luminescence was measured 6 hours after TNF-α incubation. Data are representative of 3 independent experiments (mean ± SEM; $^*P < 0.05$).

10E). In summary, SIK2, by promoting p300 Ser89 phosphorylation, protects liver from excess fat accumulation, inflammation, damage, and consequently insulin resistance, beneficial effects in obesity and type 2 diabetes.

## Discussion

In the search for a candidate kinase that plays a role in hepatocyte energy metabolism, SIK2 appeared interesting due to its abundant expression with unknown function in liver (22). SIKs share several substrates with AMPK, as in the case of Ser171 of CRTC2 (33), and have been previously implicated in the molecular control of hepatic glucose production and in protection from metabolic syndrome (23, 29, 34). In the present study, we demonstrate that SIK2 activity is inhibited in the liver in two independent mouse models of obesity and type 2 diabetes (*ob/ob* and HFD-fed mice) and consequently can be associated not only with elevated blood glucose levels (23) but also with the development of hepatic steatosis. In support of this hypothesis, using both SIK2 overexpression and knockdown approaches, we revealed its involvement in the repression of genes critical for fatty acid and TG synthesis. Importantly, we found that SIK2 overexpression protects from liver damage induced by chronic exposure to HFD during obesity and type 2 diabetes, via p300 Ser89 phosphorylation and subsequent inactivation of p300 HAT activity (Figure 8).

First, we propose that the formation of the glucose-sensing complex on glycolytic and lipogenic gene promoters may allow the coactivator p300 to form a bridge with the basal transcriptional apparatus, thus physically assisting the recruitment of RNA polymerase II, as has been previously described in other models (13). Indeed, p300 was recruited to the *L-PK* promoter in a glucose-dependent manner, promoting ChREBP as well as histone H3K9 and H4K8 acetylation. Importantly, we show here that SIK2 impacts ChREBP posttranscriptionally through the regulation of p300 HAT activity. Interestingly, increased occupancy and acetylation of ChREBP at the *L-PK* promoter after treatment with high-glucose concentrations were largely attenuated by downregulation of p300 function through SIK2-mediated Ser89 p300 phosphorylation. Taken together, our results demonstrate that p300 coactivates glucose-mediated ChREBP induction of glycolytic and lipogenic gene expression by acetylating both histone and ChREBP itself, which may contribute to increased association of ChREBP and RNA polymerase II with the promoter. Significantly, we demonstrate, for the first time to our knowledge, that acetylation of ChREBP by p300 constitutes a regulatory mechanism for ChREBP-dependent transcription. The major ChREBP acetylated site is K672 located within its DNA-binding domain. Mutation of ChREBP K672 resulted in decreased DNA binding and transactivation activity, indicating that acetylation of ChREBP is required for its capacity to interact with its target gene promoters. This observation correlates with previous reports showing that increasing acetylation within the DNA-binding domain of transcription factors such as p53 (19), Nrf2 (35), or HNF4 (36) enhances their binding to the DNA, allowing an increase in their transcriptional activity. Although K672 was identified as the major acetylation site for ChREBP, K658 and K678 were also shown to be acetylated. However, single mutation at these sites did not affect ChREBP transcriptional activity. Interestingly, recent studies demonstrated that acetylation of p53 at different lysines residues affected

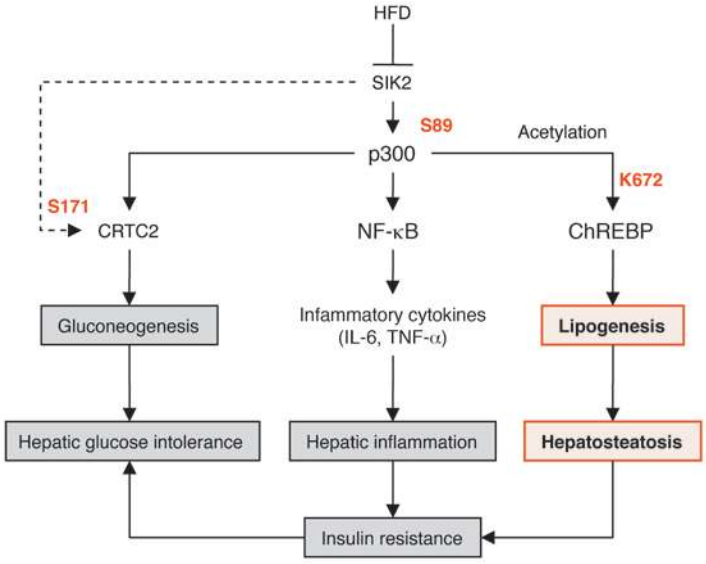


**Figure 8**
Model of SIK2 actions on the regulation of p300 HAT activity, linking dietary lipids, hepatosteatosis, hepatic inflammation, and glucose intolerance.

different biological processes. Acetylation of p53 at K120 in the DNA-binding domain is crucial for apoptosis but is dispensable for cell-cycle arrest (37). Likewise, acetylation at K658 and K678 in ChREBP may have different functional outcomes and may selectively play a role in the regulation of subsets of target genes involved in different metabolic pathways other than lipogenesis. Therefore, in the future, it will be important to determine, in states of obesity and type 2 diabetes, whether ChREBP acetylation is generally increased or whether this acetylation occurs at specific sites, allowing ChREBP to be recruited selectively to its target gene promoters.

Overall, the present results suggest that modulation of p300 HAT activity by SIK2 in liver could be an attractive approach to relieve symptoms associated with NAFLD. Hepatic de novo lipogenesis, together with expression of genes in this pathway, are increased in NAFLD patients (38). As a master regulator of fatty acid synthesis, ChREBP was suggested to be involved in the development of this disease by contributing to the onset of fatty liver phenotypes (9). Liver-specific silencing of ChREBP expression in *ob/ob* mice resulted in a decrease in liver and serum lipid levels and in an improvement in metabolic profiles (9) that are reminiscent of the phenotype resulting from inhibition of p300 function in liver of SIK2-overexpressing mice. Cotransfection of SIK2 with a non-phosphorylable form of p300 at Ser89 efficiently reversed the inhibitory effect of SIK2 on glycolytic and lipogenic genes and TG synthesis. In addition, while acetylation and deacetylation of ChREBP are dynamic processes under normal physiological conditions (Supplemental Figure 10G), so that acetylated ChREBP levels are transiently elevated in response to feeding to activate ChREBP signaling pathway in hepatocytes, constitutively elevated ChREBP acetylation levels are also associated with pathological states of hepatic steatosis (Supplemental Figure 10G). This increase in p300 HAT activity and hyperacetylation levels in state of obesity and type 2 diabetes through the decrease in SIK2 kinase activity may explain dysregulation of energy homeostasis. In this line of evidence, we show that downregulation of p300 activity, through SIK2-mediated Ser89 phosphorylation resulted in a marked decrease in expression of ChREBP target genes, which therefore decreased TG levels. Each of these changes results in improved lipid profiles that may reduce the probability of NAFLD. However, in this model, it would be interesting to determine the contribution of the transcription factor SREBP-1c, which is also regulated by acetylation in a p300-dependent manner (39). Indeed, several studies demonstrated that upregulation of SREBP-1c activity is associated with the development of hepatic steatosis (40).

Because the phosphorylation of p300 at Ser89 inhibits its intrinsic HAT activity directly, it may also affect p300 transcription coactivator function in different systems. These observations suggest that the SIK2-mediated p300 Ser89 phosphorylation may have a broader effect on the transcription events involving p300. As a consequence, the regulation of transcription pathways aside from lipogenesis by SIK2 may go through inhibiting p300 acetylation of other transcriptional factors. In this line of evidence, as previously described by Y. Liu and colleagues (26), p300 inhibition reduced expression of G6Pase and PEPCK and inhibited hepatic glucose production. Therefore, p300 downregulation contributes to decreased serum glucose levels and increased insulin sensitivity, which are beneficial effects in diabetes. In addition, concomitant with the development of hepatosteatosis, hepatic inflammation is an established risk factor for the development of hepatic insulin resistance and glucose intolerance (41), which in turn can stimulate the development and progression to hepatosteatitis (42). We showed that moderate and systemic SIK2 overexpression also results in protection from obesity-induced inflammation characterized by a decrease in IL-6 and TNF-α secretion and by an inhibition of NF-κB activity through direct regulation of p300 HAT activity. The hepatic NF-κB signaling pathway is activated by HFD exposure and triggers insulin resistance (30), thereby linking inflammation with obesity-induced insulin resistance. This observation is supported by recent findings that link p300 and inflammation. For example, it has been previously demonstrated that enhancement of p300 activity leads to the activation of the NF-κB signaling pathway and secretion of the proinflammatory cytokine IL-6 (31). Together, these finding further indicate that SIK2 also protects liver from inflammation, through the inhibition of p300 HAT activity.

However, our study did not directly address the question of the specific action of p300 Ser89 phosphorylation in the regulation of a select set of p300 substrates. Indeed, in this study, although we dissected the complexity of SIK2 action on p300 functions in the liver and studied its effects on glucose and lipid metabolism, it is possible that the inhibition of p300 function by SIK2 could still have some effects on many other processes, as revealed by previous studies (14–17). For example, our analysis confirmed that SIK2 silencing enhanced H3K9 and H4K8 acetylation in DNA isolated from the liver at the global level, but the biological relevance of this modification in metabolism is not clear and will be an interesting topic for future investigation. Although many of the changes can be secondary, some others may be directly linked to p300 Ser89 phosphorylation by SIK2, and their impact on glucose and lipid metabolism should be carefully investigated in future studies. Interestingly, p300 Ser89 is localized near an LXXLL motif. This protein-protein interaction domain has been

previously described to be important for the function of several transcription factors, such as PPARγ and FOXO1 (43, 44). Thus, it is possible that phosphorylation of p300 at Ser89 by SIK2 affects its interaction with a select set of substrates. Nevertheless, further investigation, ongoing in our laboratory, will be required to ascertain how this specificity is achieved.

Finally, today, it is well accepted that mice with type 2 diabetes manifest selective hepatic insulin resistance, characterized by an impaired suppression of gluconeogenesis, while lipogenesis, which is normally dependent on insulin action, remains fully activated, producing the deleterious combination of hyperinsulinemia, hyperglycemia, and hypertriglyceridemia. Despite the insulin-resistant state, insulin sensitivity seems to be maintained for the ChREBP pathway, with elevated fatty acid and TG synthesis in the liver. Interestingly, it was recently proposed that, independently of this state of insulin resistance, lipogenesis could also be driven by other factors in the metabolic syndrome (45). Supporting this hypothesis, in our study, SIK2 appears to be the missing link to reconcile this apparent paradox of increased lipogenesis in the state of insulin resistance. First, we recently provided evidence that SIK2 is directly activated by insulin through Ser358 Akt phosphorylation during refeeding and thus is a direct target of insulin resistance (23) (Supplemental Figure 9A). In addition, in the current study, we demonstrated that SIK2 inhibited hepatic lipogenesis in a p300/ChREBP-dependent manner. Consequently, in the state of insulin resistance, the decrease in SIK2 function enhanced p300 HAT activity and transactivation potency, which in turn promoted fatty acid synthesis despite decreased Akt activation. Thus, Akt-mediated insulin regulation of SIK2 activity appears to be a key component in the integration of both glucose and lipid metabolism in liver during fasting and feeding (Figure 8).

Therefore, taken together, our findings suggest that SIK2 activators or specific p300 inhibitors, by reducing acetylation at specific genomic regions, may offer promise for novel therapeutic approaches for treating hepatic diseases such as NAFLD as well as obesity-associated metabolic syndrome.

## Methods

See Supplemental Methods for details.

*Mouse strains and adenoviruses*. All procedures involving mice were performed in accordance with Direction départementale des services vétérinaires de Paris (Paris, France) guidelines and were approved by the Cochin Institute IACUC. Adenoviral expression vector and RNAi constructs for SIK2 shRNA (SIK2i), unspecific shRNA (USi), GFP, p300, and SIK2 were provided by M. Montminy and Y. Liu (Salk Institute for Biologicals Studies, La Jolla, California, USA; refs. 23, 26). For nutritional studies, mice were studied under fed conditions.

*Reporter assay*. The ChoRE-luc (carbohydrate response element of the L-pyruvate kinase promoter [ChoRE] luciferase) reporter gene, pNF-κBLuc (Clontech), Gal4-p300 (WT or S89A mutant), Gal4-ChREBP, and UAS5E1B-TATALUC were described previously (11, 46). The reporter constructs used were the PG5 luciferase reporter vector, which contains 5 Gal4 DNA-binding sites (PG5LUC, Promega). RSV β-galactosidase plasmid (RSV β-gal) was used as a control to normalize to DNA transfection. All of the Gal4-p300 constructs are derivatives of the pVR-1012gal4-p300 expression vector, which expressed full-length p300 fused to the Gal4-DBD as previously described (46). ChREBP DN (dominant negative ChREBP-R673A/R674G) and acetylation-defective ChREBP mutants (K658R, K672R, and K678R) were constructed using the QuikChange Site-Directed Mutagenesis Kit from Stratagene.

*Cell culture and transfection*. Mouse hepatocytes were harvested, cultured, and infected with adenoviruses as previously described (7). HEK293T and HepG2 cells were maintained and transfections carried out as previously described (23).

*MS/MS analysis*. FLAG-tagged ChREBP (FLAG-ChREBP) was expressed in HepG2 cells overexpressing p300. Acetylated FLAG-ChREBP was purified by binding to M2 agarose beads and subjected to MS/MS spectrometry analysis as described previously (47).

*ChIP analysis*. Primary hepatocytes were cultured for 18 hours in the presence of 100 nM insulin and either 5 or 25 mM glucose before cross-linking with 1% formaldehyde. ChIP assays were performed as previously described (48).

*Proteomic analysis*. SIK2 IPs were prepared from HEK293 T cells, and peptide mixtures were analyzed by multidimensional protein identification technology (MudPIT) analysis. Tandem mass spectra were searched against the most recent versions of the predicted rat, mouse, and human proteins, to which common contaminants such as keratin and trypsin were added using a modified version of the PEP_PROB algorithm (http://bart.scripps.edu/public/search/pep_probe/search.jsp). Search results were filtered and grouped using DTA Select (http://fields.scripps.edu/DTASelect/index.html).

*Statistics*. Results are expressed as mean ± SEM. Statistical significance was assessed using 1-way ANOVA. Differences were considered statistically significant at $P < 0.05$. All experiments were performed on at least 3 independent occasions.

## Acknowledgments

The authors would like to thank Anne-Françoise Burnol and Marthe Moldes (Institut Cochin, Département d'Endocrinologie, Métabolisme et Cancer, Université Paris Descartes, Paris, France) for helpful discussions; Véronique Fauveau of the Plate-Forme of "Micro-Chirurgie" (Institut Cochin, Paris, France) for performing adenoviral injections in mice; and Evelyne Souil of the "Plateforme de Morphologie/Histology" (Institut Cochin, Paris, France) for performing liver sections and oil red O staining. Mice used in this study were housed in an animal facility equipped with the help of the Région Ile de France. The work performed at the Cochin Institute was supported by grants from the Agence nationale de la recherche (ANR-09-JCJC-0057-01) and by the Fondation pour la recherche médicale.

Received for publication October 30, 2009, and accepted in revised form September 29, 2010.

Address correspondence to: Renaud Dentin, Institut Cochin, Département d'Endocrinologie, Métabolisme et Cancer, Faculté de médecine 3ème étage, 24 Rue du Faubourg Saint Jacques, 75014 Paris, France. Phone: 33.1.53.73.27.20; Fax: 33.1.53.73.27.03; E-mail: renaud.dentin@inserm.fr.

1. Eckel RH, Grundy SM, Zimmet PZ. The metabolic syndrome. *Lancet*. 2005;365(9468):1415–1428.
2. Ford ES, Giles WH, Mokdad AH. Increasing prevalence of the metabolic syndrome among U.S. adults. *Diabetes Care*. 2004;27(10):2444–2449.
3. Hirosumi J, et al. A central role for JNK in obesity and insulin resistance. *Nature*. 2002;420(6913):333–336.
4. Ozcan U, et al. Endoplasmic reticulum stress links obesity, insulin action, and type 2 diabetes. *Science*. 2004;306(5695):457–461.
5. Postic C, Girard J. Contribution of de novo fatty acid synthesis to hepatic steatosis and insulin resistance: lessons from genetically engineered mice. *J Clin Invest*. 2008;118(3):829–838.
6. Dentin R, Girard J, Postic C. Carbohydrate responsive element binding protein (ChREBP) and sterol regulatory element binding protein-1c (SREBP-1c): two key regulators of glucose metabolism and lipid

synthesis in liver. *Biochimie*. 2005;87(1):81–86.
7. Dentin R, et al. Hepatic glucokinase is required for the synergistic action of ChREBP and SREBP-1c on glycolytic and lipogenic gene expression. *J Biol Chem*. 2004;279(19):20314–20326.
8. Yamashita H, et al. A glucose-responsive transcription factor that regulates carbohydrate metabolism in the liver. *Proc Natl Acad Sci U S A*. 2001; 98(16):9116–9121.
9. Dentin R, et al. Liver-specific inhibition of ChREBP improves hepatic steatosis and insulin resistance in ob/ob mice. *Diabetes*. 2006;55(8):2159–2170.
10. Iizuka K, Bruick RK, Liang G, Horton JD, Uyeda K. Deficiency of carbohydrate response element-binding protein (ChREBP) reduces lipogenesis as well as glycolysis. *Proc Natl Acad Sci U S A*. 2004; 101(19):7281–7286.
11. Burke SJ, Collier JJ, Scott DK. cAMP prevents glucose–mediated modifications of histone H3 and recruitment of the RNA polymerase II holoenzyme to the L–PK gene promoter. *J Mol Biol*. 2009; 392(3):578–588.
12. Barrera LO, Ren B. The transcriptional regulatory code of eukaryotic cells--insights from genome-wide analysis of chromatin organization and transcription factor binding. *Curr Opin Cell Biol*. 2006; 18(3):291–298.
13. Chan HM, La Thangue NB. p300/CBP proteins: HATs for transcriptional bridges and scaffolds. *J Cell Sci*. 2001;114(pt 13):2363–2373.
14. Yao TP, et al. Gene dosage-dependent embryonic development and proliferation defects in mice lacking the transcriptional integrator p300. *Cell*. 1998; 93(3):361–372.
15. Kaur H, Chen S, Xin X, Chiu J, Khan ZA, Chakrabarti S. Diabetes-induced extracellular matrix protein expression is mediated by transcription coactivator p300. *Diabetes*. 2006;55(11):3104–3111.
16. Gayther SA, et al. Mutations truncating the EP300 acetylase in human cancers. *Nat Genet*. 2000; 24(3):300–303.
17. Gusterson RJ, Jazrawi E, Adcock IM, Latchman DS. The transcriptional co-activators CREB-binding protein (CBP) and p300 play a critical role in cardiac hypertrophy that is dependent on their histone acetyltransferase activity. *J Biol Chem*. 2003; 278(9):6838–6847.
18. Fu M, et al. Acetylation of androgen receptor enhances coactivator binding and promotes prostate cancer cell growth. *Mol Cell Biol*. 2003;23(23):8563–8575.
19. Gu W, Roeder RG. Activation of p53 sequence-specific DNA binding by acetylation of the p53 C-terminal domain. *Cell*. 1997;90(4):595–606.
20. Yuan LW, Soh JW, Weinstein IB. Inhibition of histone acetyltransferase function of p300 by PKCdelta. *Biochim Biophys Acta*. 2002;1592(2):205–211.
21. Yuan LW, Gambee JE. Phosphorylation of p300 at serine 89 by protein kinase C. *J Biol Chem*. 2000; 275(52):40946–40951.
22. Okamoto M, Takemori H, Katoh Y. Salt-inducible kinase in steroidogenesis and adipogenesis. *Trends Endocrinol Metab*. 2004;15(1):21–26.
23. Dentin R, et al. Insulin modulates gluconeogenesis by inhibition of the coactivator TORC2. *Nature*. 2007;449(7160):366–369.
24. Weisberg SP, McCann D, Desai M, Rosenbaum M, Leibel RL, Ferrante AW Jr. Obesity is associated with macrophage accumulation in adipose tissue. *J Clin Invest*. 2003;112(12):1796–1808.
25. Wellen KE, Hatzivassiliou G, Sachdeva UM, Bui TV, Cross JR, Thompson CB. ATP-citrate lyase links cellular metabolism to histone acetylation. *Science*. 2009; 324(5930):1076–1080.
26. Liu Y, et al. A fasting inducible switch modulates gluconeogenesis via activator/coactivator exchange. *Nature*. 2008;456(7219):269–273.
27. Chen H, Tini M, Evans RM. HATs on and beyond chromatin. *Curr Opin Cell Biol*. 2001;13(2):218–224.
28. Tsatsos NG, Davies MN, O'Callaghan BL, Towle HC. Identification and function of phosphorylation in the glucose-regulated transcription factor ChREBP. *Biochem J*. 2008;411(2):261–270.
29. Horike N, et al. Adipose-specific expression, phosphorylation of Ser794 in insulin receptor substrate-1, and activation in diabetic animals of salt-inducible kinase-2. *J Biol Chem*. 2003;278(20):18440–18447.
30. Cai D, et al. Local and systemic insulin resistance resulting from hepatic activation of IKK-beta and NF-kappaB. *Nat Med*. 2005;11(2):183–190.
31. Bourguignon LY, Xia W, Wong G. Hyaluronan-mediated CD44 interaction with p300 and SIRT1 regulates beta-catenin signaling and NFkappaB-specific transcription activity leading to MDR1 and Bcl-xL gene expression and chemoresistance in breast tumor cells. *J Biol Chem*. 2009;284(5):2657–2671.
32. Ndlovu N., et al. Hyperactivated NF{kappa}B and AP1 transcription factors promote highly accessible chromatin and constitutive transcription across the IL6 gene promoter in metastatic breast cancer cells. *Mol Cell Biol*. 2009;29(20):5488–5504.
33. Conkright MD, et al. TORCs: transducers of regulated CREB activity. *Mol Cell*. 2003;12(2):413–423.
34. Yoon YS, Seo WY, Lee MW, Kim ST, Koo SH. Salt-inducible kinase regulates hepatic lipogenesis by controlling SREBP-1c phosphorylation. *J Biol Chem*. 2009;284(16):10446–10452.
35. Sun Z, Chin YE, Zhang DD. Acetylation of Nrf2 by p300/CBP augments promoter-specific DNA binding of Nrf2 during the antioxidant response. *Mol Cell Biol*. 2009;29(10):2658–2672.
36. Soutoglou E, Katrakili N, Talianidis I. Acetylation regulates transcription factor activity at multiple levels. *Mol Cell*. 2000;5(4):745–751.
37. Tang Y, Luo J, Zhang W, Gu W. Tip60-dependent acetylation of p53 modulates the decision between cell-cycle arrest and apoptosis. *Mol Cell*. 2006; 24(6):827–839.
38. Donnelly KL, Smith CI, Schwarzenberg SJ, Jessurun J, Boldt MD, Parks EJ. Sources of fatty acids stored in liver and secreted via lipoproteins in patients with nonalcoholic fatty liver disease. *J Clin Invest*. 2005; 115(5):1343–1351.
39. Giandomenico V, Simonsson M, Gronroos E, Ericsson J. Coactivator-dependent acetylation stabilizes members of the SREBP family of transcription factors. *Mol Cell Biol*. 2003;23(7):2587–2599.
40. Yahagi N, et al. Absence of sterol regulatory element-binding protein-1 (SREBP-1) ameliorates fatty livers but not obesity or insulin resistance in Lep(ob)/Lep(ob) mice. *J Biol Chem*. 2002; 277(22):19353–19357.
41. Shoelson SE, Herrero L, Naaz A. Obesity, inflammation, and insulin resistance. *Gastroenterology*. 2007; 132(6):2169–2180.
42. Ota T, et al. Insulin resistance accelerates a dietary rat model of nonalcoholic steatohepatitis. *Gastroenterology*. 2007;132(1):282–293.
43. Nakae J, et al. The LXXLL motif of murine forkhead transcription factor FoxO1 mediates Sirt1-dependent transcriptional activity. *J Clin Invest*. 2006; 116(9):2473–2483.
44. Chen S, et al. Both coactivator LXXLL motif-dependent and -independent interactions are required for peroxisome proliferator-activated receptor gamma (PPARgamma) function. *J Biol Chem*. 2000; 275(6):3733–3736.
45. Kammoun HL, et al. GRP78 expression inhibits insulin and ER stress-induced SREBP-1c activation and reduces hepatic steatosis in mice. *J Clin Invest*. 2009;119(5):1201–1215.
46. Yang W, Hong YH, Shen XQ, Frankowski C, Camp HS, Leff T. Regulation of transcription by AMP-activated protein kinase: phosphorylation of p300 blocks its interaction with nuclear receptors. *J Biol Chem*. 2001;276(42):38341–38344.
47. Miao J, et al. Bile acid signaling pathways increase stability of small heterodimer partner (SHP) by inhibiting ubiquitin-proteasomal degradation. *Genes Dev*. 2009;23(8):986–996.
48. Dentin R, Hedrick S, Xie J, Yates J 3rd, Montminy M. Hepatic glucose sensing via the CREB coactivator CRTC2. *Science*. 2008;319(5868):1402–1405.